Dynamical calculations of the above-barrier heavy-ion fusion cross sections using Hartree-Fock nuclear densities with the SKX coefficient set

M. V. Chushnyakova,[1,2] R. Bhattacharya,[3] and I. I. Gontchar[4]
[1]*Department of Physics, Omsk State Technical University, Omsk, Russia*
[2]*Department of Applied Physics, Tomsk Polytechnic University, Tomsk, Russia*
[3]*Department of Physics, University of Calcutta, Kolkata, India*
[4]*Department of Physics and Chemistry, Omsk State Transport University, Omsk, Russia*
(Received 4 May 2014; published 21 July 2014)

Background: In our previous paper [Gontchar *et al.*, Phys. Rev. C **89**, 034601 (2014)] we have calculated the capture (fusion) excitation functions for several reactions with ^{16}O, ^{28}Si, and ^{32}S nuclei as the projectiles and ^{92}Zr, ^{144}Sm, and ^{208}Pb nuclei as the targets. These calculations were performed by using our fluctuation-dissipation trajectory model based on the double-folding approach with the density-dependent M3Y *NN* forces that include the finite range exchange part. For the nuclear matter density the Hartree-Fock approach with the SKP coefficient set that includes the tensor interaction was applied. It was found that for most of the reactions induced by ^{16}O the calculated cross sections cannot be brought into agreement with the data. This suggested that the deviation in the calculated nuclear density for ^{16}O from the experimental one was crucial.
Method: The SKX parameter set is used to obtain the nuclear densities. Reactions with ^{12}C and ^{36}S as the projectiles and ^{204}Pb as the target are included in the analysis in addition to those of the previous paper. Only data that correspond to the collision energy $E_{\rm c.m.} > 1.1U_{B0}$ (U_{B0} is the s-wave fusion barrier height) are included in the analysis. The radial friction strength K_R is used as the individual adjustable parameter for each reaction.
Results: For all 13 reactions (91 points) it is possible to reach an agreement with the experimental fusion cross sections within 10%. Only at ten points does the deviation exceed 5%. The value of K_R, which provides the best agreement with the data in general, decreases as the system gets heavier in accord with the previous paper [Gontchar *et al.*, Phys. Rev. C **89**, 034601 (2014)]. A universal analytical approximation for the dependence of K_R upon the Coulomb barrier height is found.
Conclusions: The developed model is able to reproduce the above-barrier portion of the fusion excitation function within 5% with a probability of 90%. Only one fitting parameter per excitation function K_R is used. The model can be used to predict the results of relevant measurements. The universal analytical approximation of the K_R dependence upon the Coulomb barrier height helps to find the starting value of K_R for a more accurate description.

DOI: 10.1103/PhysRevC.90.017603 PACS number(s): 25.70.Jj, 25.60.Pj, 24.10.−i

I. INTRODUCTION

It was proved that accounting for coupling to the collective modes in the target and projectile nuclei is vital for describing the modern precision experimental data on the heavy-ion capture cross sections σ at the near- and below-barrier energies [1,2]. Yet at the well-above-barrier energies these couplings became unimportant, and the data were analyzed within the framework of the barrier penetration model (BPM) [3] and of the trajectory fluctuation-dissipation model (TFDM) [4,5]. In Ref. [3] it was shown that within the BPM the abnormally large values of the diffuseness of the Woods-Saxon nucleus-nucleus potential $a_{\rm WS}$ were required to reproduce the experimental capture cross sections. It was pointed out in Ref. [3] that a new model for the capture process was needed. In Refs. [5,6] such a model was developed. In the model, the fictitious particle with the reduced mass moves under the action of the conservative, dissipative, and stochastic forces. Only the collision process at the energies well above the Coulomb barrier,

$$B_Z = Z_P Z_T / \left(A_P^{1/3} + A_T^{1/3}\right) \text{ MeV} \qquad (1)$$

is considered, therefore there is no need to account for quantum effects, such as tunneling and channel coupling. The nucleus-nucleus potential is calculated with the help of the double-folding approach with the density-dependent M3Y *NN* forces that include the finite range exchange part [7]. The code DFMSPH [8] is used for this purpose. Comprehensive descriptions of the TFDM and all its ingredients can be found in Refs. [4–6,8]. The SKP Hartree-Fock approach [9] that included the tensor interaction [10,11] was applied in Ref. [4] for the nuclear matter density, which was the crucial ingredient of the double-folding approach. It was found in Ref. [4] that for most of the reactions induced by ^{16}O the calculated cross sections cannot be brought into agreement with the data. This was attributed to the deviation in the calculated nuclear density for ^{16}O from the experimental one.

II. RESULTS

In the present Brief Report we repeat the analysis of Ref. [4] with the nuclear densities obtained by using the SKX parameter set [12]. All other parameters in the present Brief Report remain the same as in Ref. [4]. In Table I we represent the deviation of the calculated rms charge radii $R_{q\rm th}$ from the experimental ones $R_{q\ \rm expt.}$ taken from Ref. [13]. One sees that the SKX parameter set provides much better agreement with the data for the light nuclei. This encourages us to hope that it is

TABLE I. The deviation in the calculated rms charge radii $R_{q\text{th}}$ from the experimental ones $R_{q\ \text{expt.}}$ taken from Ref. [13]. Results for the SKP parameter set for the nuclei not involved in Ref. [4] are not shown.

Nucleus	^{12}C	^{16}O	^{28}Si	^{32}S	^{36}S	^{92}Zr	^{144}Sm	^{204}Pb	^{208}Pb
$R_{q\text{th}}/R_{q\ \text{expt.}}$ SKP [4]		1.0499	1.0193	1.0270		1.006	1.005		0.9996
$R_{q\text{th}}/R_{q\ \text{expt.}}$ SKX this Brief Report	1.0199	1.0164	1.0029	0.9987	1.0006	0.9952	0.9994	0.9985	0.9981

possible to reach better agreement with the fusion data than in Ref. [4], in particular for the reactions induced by ^{12}C and ^{16}O.

In Table II a list of reactions is presented for which the calculations have been performed. We see that the fusion barriers obtained with the SKX parameters are always higher than those of Ref. [4] obtained with the SKP parameters. This probably is somewhat surprising because the rms charge radii of the nuclei differ only slightly. However, one should keep in mind that, due to the short-range character of the nuclear interaction, this is the tail of the matter density distribution which is important for the potential.

In Ref. [4] we have found that the radial friction strength coefficient that provides the best agreement with the fusion data depends upon the system. By following this finding, we vary the value of K_R by searching for the minimal value of χ^2_σ averaged over the number of points v,$\chi^2_{v\sigma}$,

$$\chi^2_{v\sigma} = \frac{1}{v}\sum_{i=1}^{v}\left(\frac{\sigma_{i\text{th}} - \sigma_{i\ \text{expt.}}}{\Delta\sigma_{i\ \text{expt.}}}\right)^2. \qquad (2)$$

Here $\sigma_{i\,\text{th}}$ is the theoretical value of the cross section at the particular value of $E_{\text{c.m.}\,i}$, and $\sigma_{i\ \text{expt.}}$ and $\Delta\sigma_{i\ \text{expt.}}$ are the experimental values of the cross section and its error at the same energy. The resulting cross sections divided by the experimental ones $\xi = \sigma_{\text{th}}/\sigma_{\text{expt.}}$ are shown in Fig. 1, which is to be compared with Fig. 8 of Ref. [4]. The values of K_R that provide the minimal $\chi^2_{v\sigma}$ values K_{Rm} are indicated in the figure. All 13 reactions are split into four groups according to the projectile nucleus; results for each group are shown in separate panels. For all reactions (91 points) it is possible to reach an agreement with the data within 10%. Only at ten points does the deviation exceed 5%.

In Ref. [4] for all the reactions induced by ^{16}O the theoretical description of the data was poor except for ^{16}O + ^{208}Pb. Now we see that for ^{16}O + ^{208}Pb this was most likely the occasional cancellation of several inaccuracies (one of which was poor matter density for ^{16}O). In Fig. 1(b) we see that ξ for this reaction behaves in an odd manner. This could be expected by keeping in mind the discussion of this reaction in the Introduction of Ref. [3] and in Ref. [14]. This reaction was one of few (if not the only one) for which in Ref. [14] no reasonable fit of the above- and below-barrier data was reached with the same diffuseness of the Woods-Saxon nucleus-nucleus potential. By considering Figs. 1(a), 1(b), and 1(d) more attentively one can see a similarity in the behavior of ξ for the reactions with ^{208}Pb (circles). On the other hand, the data for the ^{36}S + ^{208}Pb reaction [Fig. 1(d)] deviate from all other reactions: All four circles in this figure are beyond the 5% stripe. It should be noted that this is one of two reactions for which the data were obtained at a laboratory different from the Australian National University.

Let us focus now on the values of the radial friction strength coefficient K_{Rm} indicated in the figure. This value decreases in each panel, in general, as the Coulomb barrier height increases in accord with the previous paper.

TABLE II. Parameters of the potentials for the reactions under consideration: B_Z [Eq. (1)]; $U_{B0\ \text{expt.}}$ and $R_{B0\ \text{expt.}}$ are taken from Ref. [3] where they were extracted from the fusion data analysis. U_{B0} and R_{B0} are the potential barrier height and radius obtained in Ref. [4] (SKP) and in the present calculations (SKX). The last two columns contain the references to the papers where the corresponding fusion excitation function was measured and the number of data points invoked for our analysis. Note that, in many cases, data from Ref. [15] are used.

Reaction	B_Z (MeV)	$U_{B0\ \text{expt.}}$ (MeV)	$R_{B0\ \text{expt.}}$ (fm)	SKP U_{B0} (MeV)	SKP R_{B0} (fm)	SKX U_{B0} (MeV)	SKX R_{B0} (fm)	Expt. data Refs.	Number of data points
^{12}C + ^{92}Zr	35.27	32.31	9.68			31.9	10.17	[16]	7
^{12}C + ^{144}Sm	49.4					49.4	10.87	[17]	4
^{12}C + ^{208}Pb	59.89					57.8	11.63	[18]	7
^{12}C + ^{204}Pb	60.17	57.55	11.34			58.0	11.57	[19]	8
^{16}O + ^{92}Zr	45.49	41.96	10.02	40.9	10.56	41.6	10.41	[16]	18
^{16}O + ^{144}Sm	63.91	61.03	10.85	59.8	11.24	60.8	11.11	[20]	7
^{16}O + ^{208}Pb	77.68	74.52	11.31	74.7	11.95	75.7	11.83	[14]	8
^{16}O + ^{204}Pb	78.03					76.1	11.78	[21]	2
^{28}Si + ^{92}Zr	74.16	70.93	10.19	69.7	10.84	70.6	10.73	[16]	6
^{28}Si + ^{208}Pb	128.1	128.07	11.45	127.7	12.23	128.8	12.17	[22]	10
^{36}S + ^{208}Pb	142.19					143.2	12.54	[23]	4
^{36}S + ^{204}Pb	142.78					143.9	12.49	[24]	6
^{32}S + ^{208}Pb	144.18	144.03	10.91	143.9	12.39	145.7	12.31	[22]	4

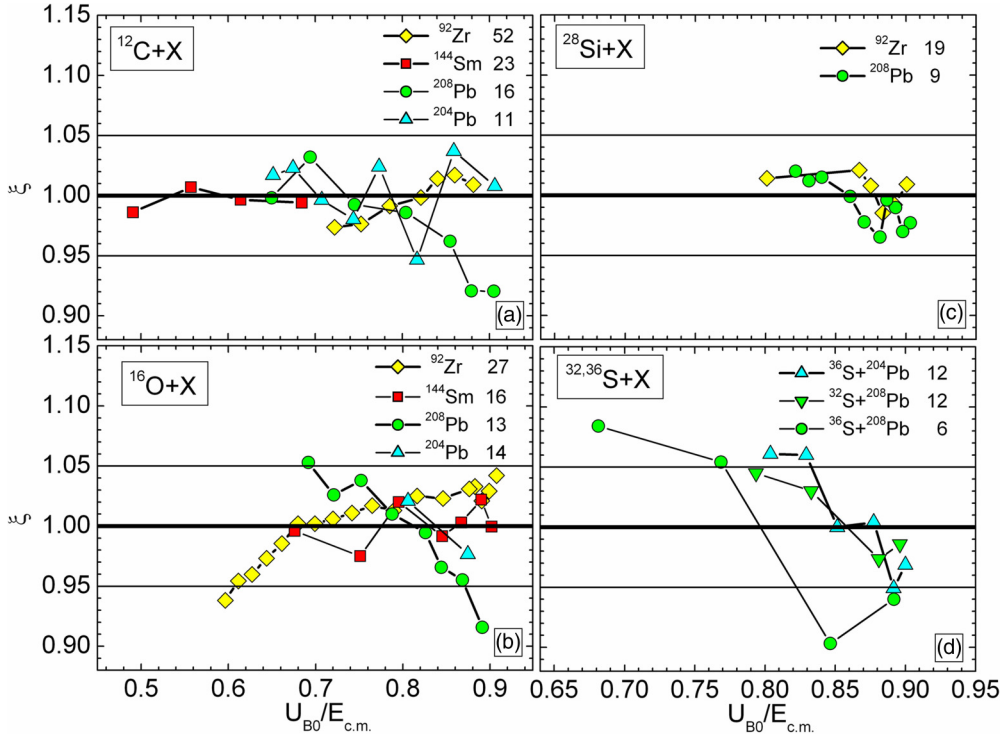

FIG. 1. (Color online) The ratio $\xi = \sigma_{\rm th}/\sigma_{\rm expt.}$ as the function of $U_{B0}/E_{\rm c.m.}$ for 13 reactions listed in Table II. All reactions are split into four groups according to the projectile nucleus. These calculations were performed with the values of K_R (shown in the figures in units of zs GeV^{-1}), which provide the minimum value of $\chi^2_{v\sigma}$ for each reaction.

In Fig. 2 the values of K_{Rm} for all reactions are presented versus B_Z (symbols). The general trend for K_{Rm} to decrease as B_Z increases is reproduced by the empirical formula,

$$K_{\rm Re} = K_1 \exp\left(\frac{B_0 - B_Z}{\Delta B}\right) + K_0, \qquad (3)$$

where $K_1 = 260$ zs GeV^{-1}, $K_0 = 10$ zs GeV^{-1}, $B_0 = 7$ MeV, and $\Delta B = 15$ MeV with $\chi^2_{vK} = 10$. Here

$$\chi^2_{vK} = \frac{1}{13}\sum_{i=1}^{13}\left(\frac{K_{\rm Re} - K_{Rmi}}{\Delta K_R}\right)^2. \qquad (4)$$

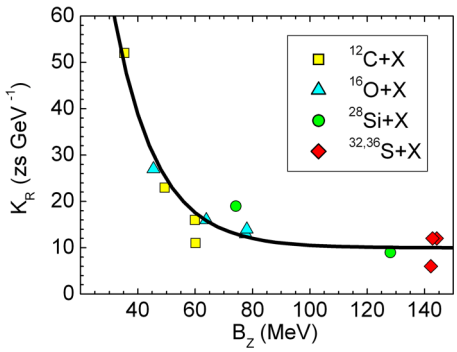

FIG. 2. (Color online) The value of the radial friction strength that provides the minimal $\chi^2_{v\sigma}$ versus B_Z (symbols). The line represents $K_{\rm Re}(B_Z)$ defined by Eq. (3).

The error of K_{Rm} was taken to be equal to the step of the K_R variation when searching for the minimum of $\chi^2_{v\sigma}$: $\Delta K_R = 1$ zs GeV^{-1}.

III. CONCLUSIONS

The developed model is able to reproduce the above-barrier portion of the experimental fusion excitation function within 5% with the probability of 90%. Only one fitting parameter per excitation function, K_R, is used. The model can be used to predict the results of relevant measurements (the data for the following reactions are missing in the literature: ^{28}Si + ^{144}Sm, ^{204}Pb; ^{32}S + ^{144}Sm, ^{92}Zr, ^{204}Pb; ^{36}S + ^{144}Sm, ^{92}Zr).

The universal analytical approximation (3) of the K_R dependence upon the Coulomb barrier height can be helpful in finding the starting value of K_R for a more accurate description.

Presently, we do not have a physical explanation for the decrease in the K_{Rm} value with B_Z. However, one has to keep in mind that the friction coefficient in the dissipative force (see Eq. (6a) of Ref. [4] or Eq. (3b) of Ref. [6]) is defined not only by its strength K_R, but also by the form factor which becomes larger due to a relatively smaller barrier radius for the reactions with larger values of B_Z.

ACKNOWLEDGMENTS

M.V.C. is grateful to the Dmitry Zimin "Dynasty" Foundation for financial support.

[1] M. Dasgupta, D. J. Hinde, N. Rowley, and A. M. Stefanini, Annu. Rev. Nucl. Part. Sci. **48**, 401 (1998).
[2] K. Hagino, N. Rowley, and A. T. Kruppa, Comput. Phys. Commun. **123**, 143 (1999).
[3] J. O. Newton, R. D. Butt, M. Dasgupta, D. J. Hinde, I. I. Gontchar, C. R. Morton, and K. Hagino, Phys. Rev. C **70**, 024605 (2004).
[4] I. I. Gontchar, R. Bhattacharya, and M. V. Chushnyakova, Phys. Rev. C **89**, 034601 (2014).
[5] M. V. Chushnyakova and I. I. Gontchar, Phys. Rev. C **87**, 014614 (2013).
[6] M. V. Chushnyakova and I. I. Gontchar, J. Phys. G: Nucl. Part. Phys. **40**, 095108 (2013).
[7] D. T. Khoa, G. R. Satchler, and W. von Oertzen, Phys. Rev. C **56**, 954 (1997).
[8] I. I. Gontchar and M. V. Chushnyakova, Comput. Phys. Commun. **181**, 168 (2010).
[9] J. Dobaczewski, H. Flocard, and J. Treiner, Nucl. Phys. A **422**, 103 (1984).
[10] R. Bhattacharya, Nucl. Phys. A **913**, 1 (2013).
[11] R. Bhattacharya, J. Mod. Phys. **4**, 33 (2013).
[12] B. A. Brown, Phys. Rev. C **58**, 220 (1998).
[13] I. Angeli, At. Data Nucl. Data Tables **87**, 185 (2004).
[14] C. R. Morton, A. C. Berriman, M. Dasgupta, D. J. Hinde, J. O. Newton, K. Hagino, and I. J. Thompson, Phys. Rev. C **60**, 044608 (1999).
[15] http://nrv.jinr.ru/nrv/webnrv/fusion/reactions.php
[16] J. O. Newton, C. R. Morton, M. Dasgupta, J. R. Leigh, J. C. Mein, D. J. Hinde, H. Timmers, and K. Hagino, Phys. Rev. C **64**, 064608 (2001).
[17] R. Kossakowski, J. Jastrzebski, P. Rymuza, W. Skulski, A. Gizon, S. André, J. Genevey, J. Gizon, and V. Barci, Phys. Rev. C **32**, 1612 (1985).
[18] A. Mukherjee, D. J. Hinde, M. Dasgupta, K. Hagino, J. O. Newton, and R. D. Butt, Phys. Rev. C **75**, 044608 (2007).
[19] A. C. Berriman, D. J. Hinde, M. Dasgupta, C. R. Morton, R. D. Butt, and J. O. Newton, Nature (London) **413**, 144 (2001).
[20] J. R. Leigh, M. Dasgupta, D. J. Hinde, J. C. Mein, C. R. Morton, R. C. Lemmon, J. P. Lestone, J. O. Newton, H. Timmers, J. X. Wei, and N. Rowley, Phys. Rev. C **52**, 3151 (1995).
[21] M. Dasgupta, D. J. Hinde, A. Diaz-Torres, B. Bouriquet, C. I. Low, G. J. Milburn, and J. O. Newton, Phys. Rev. Lett. **99**, 192701 (2007).
[22] D. J. Hinde, C. R. Morton, M. Dasgupta, J. R. Leigh, J. C. Mein, and H. Timmers, Nucl. Phys. A **592**, 271 (1995).
[23] R. Yanez, W. Loveland, A. M. Vinodkumar, P. H. Sprunger, L. Prisbrey, D. Peterson, S. Zhu, J. J. Kolata, A. Villano, and J. F. Liang, Phys. Rev. C **82**, 054615 (2010).
[24] D. J. Hinde, M. Dasgupta, N. Herrald, R. G. Nielson, J. O. Newton, and M. A. Lane, Phys. Rev. C **75**, 054603 (2007).